CLEAVAGE FRACTURE IN AS-QUENCHED 50D STEEL

W. Zhou and J. F. Knott †

The cleavage fracture of a lath martensite microstructure of 50D steel in the as-quenched condition has been established as tensile-stress controlled. Direct fractographic evidence has been obtained to show that the fracture is inclusion-related. The inclusions were observed to initiate fracture by decohering from the matrix rather than by cracking. A tentative fracture model has been proposed in which the role of an inclusion is considered to be that of a stress-concentrator, which raises the local stress level to a value sufficied to initiate fracture from autotempered carbides around the inclusion rather than providing microcracks to initiate fracture directly.

INTRODUCTION

Cleavage fracture micromechanisms in lath martensite are still relatively poorly understood. Martensitic packets (1), undissolved precipitates (2), inclusions (3) and precipitated carbides (4–5) have all been considered to be the possible sites for cleavage initiation. However, the majority of these conclusions have been inferred from correlations of microstructures with mechanical properties and little direct fractographic evidence has been obtained to support them. The present research has been carried out with the specific aim of providing fractographic information on the fracture initiation site. The cleavage fracture of a lath martensite microstructure in as-quenched condition is considered in this paper. Such microstructures may exist in the heat-affected zones after welding and before stress relief.

EXPERIMENTAL PROCEDURE AND RESULTS

Material, Heat Treatment and Metallography

The material used in the investigation was a carbon–manganese (C–Mn) structural steel conforming to the BS4360 50D specification. The chemical

† Department of Materials Science and Metallurgy, University of Cambridge, Pembroke Sreet, Cambridge CB2 3QZ, U.K.

composition of the steel is given as follows in wt.%: 0.1 C, 1.5 Mn, 0.38 Si, 0.04 Al, 0.03 Nb, 0.01 V, 0.016 P and 0.002 S. The heat treatment of the material involved austenitizing for 1 hour at 1200 °C followed by oil-quenching. Observation of nital-etched polished samples revealed a typical lath martensite microstructure as shown in Fig. 1a. Inclusion bands were observed in the rolling direction when polished samples were etched in hot picric acid. The inclusions in the bands were mainly manganese sulphides and niobium carbonitrides, as determined by energy dispersive x-ray micro-analysis (EDAX). Oxide particles were observed aligned in arrays parallel to the rolling direction in and outside the bands. Fig. 1b shows some manganese sulphides observed in the as-quenched microstructure. It can be seen from this figure that these inclusions were debonded from the matrix.

Mechanical Testing and Fractography

Seven notched specimens for microscopic fracture stress (σ_f) testing, numbered as M1–M7, were machined in the transverse-longitudinal (T–L) orientation. The geometry of the specimens was essentially the same as that of the specimens analysed by Griffiths and Owen (6) except that the thickness was 10 mm rather than 12.7 mm. These notched specimens were tested in four point bend on a Mand servo-hydraulic testing machine of 100 KN capacity at a ramp rate of 1 mm/min over the temperature range −196 to −100 °C. The fracture load of each specimen was recorded. Standard Hounsfield number 13 tensile specimens were tested on a Mand screw-driven testing machine of 50 KN capacity at the same ramp rate over the same temperature range to obtain values of yield stress (σ_y). All the specimens tested were machined to the final sizes after heat treatment to remove possible oxidation layers and quenching cracks. The values of σ_f were calculated from the values of fracture load and σ_y using the finite element analysis due to Griffiths and Owen (6). The distances (x_m) between the maximum tensile stresses ($\sigma_{11(max)}$) at fracture and the notch roots were also obtained using the same analysis. The values obtained for σ_y, σ_f and x_m are summarized in TABLE 1.

An extensive fractographic observation was carried out on the fracture surfaces of all the notched specimens using a CamScan series 4 scanning electron microscope (SEM) operated at 30 KV with a beam current of 140–180 μA. The mode of fracture for all the specimens was predominately transgranular cleavage. Many tear ridges were observed on the fracture surfaces. Some of them were several thousands of μm in length. The tear ridges, especially the long ones were usually directional when viewed at low magnifications (about 20 times) in the SEM. A significant fractographic finding is that, with the help of the directional tear ridges, general fracture initiation sites were observed below the notch roots in all the notched specimens except specimen M1. The term "general initiation site" refers to the location from which the unstable fracture of *the entire specimen* was triggered. The distances (x_i) between the general initiation sites and the notch roots were measured on the SEM fractographs and are listed in TABLE 1. Inclusions were observed in three of the six general initiation sites,

as shown in Figs. 2–4. These inclusions were identified by the EDAX to be manganese sulphides in specimen M2 (Fig. 2), niobium carbonitrides in specimen M3 (Fig. 3) and silicate in specimen M4 (Fig. 4).

TABLE 1 – Results of Mechanical Testing and Fractography

Specimen	T, °C	σ_y, MPa	σ_f, MPa	x_m, μm	x_i, μm
M1	−196	1312	2490	240	*
M2	−196	1312	2675	280	210
M3	−165	1225	2615	310	370
M4	−160	1211	2585	320	500
M5	−130	1160	2600	380	420–500
M6	−110	1118	2625	430	370–450
M7	−100	1098	2630	470	500–550

* No general initiation site was observed in specimen M1

DISCUSSION

It can be seen clearly from TABLE 1 that in the whole test temperature range −196 to −100 °C, σ_f is independent of temperature and has a constant value of 2600±110 MPa. This supports a tensile stress controlled fracture mechanism. It can also be seen from this table that the values of x_i are close to those of x_m. This indicates that the general fracture initiation sites are close to the positions of the maximum tensile stresses at fracture, further confirming that the fracture is tensile stress controlled.

Inclusions were identified in the general initiation sites of three of the seven notched specimens tested, indicating that the cleavage fracture of the as-quenched lath martensite microstructure is inclusion-related. It has been demonstrated by Tweed and Knott (7–8) and McRobie and Knott (9) that in C–Mn weld metals the cleavage fracture is inclusion-related and that the critical stage of fracture is the propagation of the nuclei of cracked inclusions into the matrix. It is questionable, however, if this fracture model can be extended to the present study. First, in this research the inclusions were observed to initiate fracture by decohering from the matrix, as can be seen from Figs. 2–4 rather than by cracking in two to provide cleavage nuclei. Second, careful study showed that the inclusions in the initiation sites of specimens M2, M3 and M4 were two or three times different in size, so, assuming that the inclusion size controlled fracture, the values of σ_f in the three specimens would be expected to be markedly different according to the Griffith equation:

$$\sigma_f = \left(\frac{4E\gamma_p}{\pi(1-\nu^2)x} \right)^{\frac{1}{2}} \tag{1}$$

where E is Young's modulus (206 GPa), ν is Possion's ratio (0.3), and x is the length of microcrack (of through-thickness type). But in fact the values of σ_f of specimens M2, M3 and M4 were approximately the same (TABLE 1). The fact that all the notched specimens had similar values of σ_f whether or not inclusions were found in the initiation sites, and disregarding the sizes of the inclusions in the initiation sites, indicates that the fracture was related not only to the inclusions but also to further microstructural features in the matrix, and that the inclusions initiated cleavage indirectly. A possible model for the fracture process is that the inclusions act as stress raisers and that the autotempered carbides around them crack to provide cleavage nuclei, the critical stage of fracture being the propagation of these cleavage nuclei into the matrix. Further study on this model requires a knowledge of the stress fields around the inclusions, the autotempered carbide size distribution and the value of γ_p. For the purpose of demonstration, if the stress concentrator of the inclusions is taken to be 3 as that of a cylindrical cavity (10) and the value of γ_p is taken to be 6 Jm^{-2}, then according to the Griffith equation a microcrack of the size of 0.03 μm might initiate fracture. Research on A533B steel (4–5) indicates that the widths of the largest autotempered carbides can be in the range of 0.03 to 0.035 μm, lending plausibility to the fracture model. According to the model, σ_f is determined by the shape of inclusions and the widths of the coarsest autotempered carbides. This model is proposed only tentatively and needs to be further examined and refined.

CONCLUSIONS

(1) The cleavage fracture stress is independent of temperature over the temperature range −196 to −100 °C. The positions of the general initiation sites are coincident with those of the maximum tensile stresses at failure. This evidence strongly indicates that the cleavage fracture of the as-quenched lath martensite microstructure is tensile-stress controlled.

(2) Direct fractographic evidence has been obtained to show that the fracture is inclusion-related. Manganese sulphides, niobium carbonitrides and silicate were identified in the initiation sites, but no oxide particles were found to initiate fracture. The inclusions were observed to initiate fracture by decohering from the matrix rather than by cracking.

(3) It is likely that the autotempered carbides cracked to provide cleavage nuclei, which propagated under a critical tensile stress. The critical tensile stress was attained because the inclusions acted as stress raisers.

SYMBOLS USED

E =Young's modulus (206 GPa)
T =test temperature (°C)
x =length of microcrack

x_i =distance between the general initiation sites and the notch root
x_m =distance of $\sigma_{11(max)}$ at fracture away from the notch root
$\sigma_{11(max)}$ =maximum tensile stress below the notch root
σ_f =microscopic cleavage fracture stress (MPa)
σ_y =yield stress (MPa)
ν =Poisson's ratio (0.3)
γ_p =effective surface energy (Jm^{-2})

ACKNOWLEDGEMENTS

The authors wish to thank Prof. D. Hull, FEng, FRS for provision of research facilities. Financial support for one of the authors (WZ) by the Chinese and British governments and Sir Y. K. Pao through a scholarship administrated by the British Council is gratefully acknowledged.

REFERENCES

(1) Dolby, R.E. and Knott, J.F., J.I.S.I., Vol. 210, 1972, pp. 857–865.

(2) Youngblood, J.L. and Raghavan, M., Metall. Trans. A, Vol. 8A, 1977, pp. 1439–1448.

(3) Bowen, P. and Knott, J.F., Met. Sci., Vol. 18, 1984, pp. 225–235.

(4) Bowen, P., Druce, S. G. and Knott, J.F., Acta Metall., Vol. 34, 1986, pp. 1121–1131.

(5) Bowen, P., Druce, S. G. and Knott, J.F., Acta Metall., Vol. 35, 1987, pp. 1735–1746.

(6) Griffiths, J.R. and Owen, D.R.J., J. Mech. Phys. Solids, Vol. 19, 1971, p. 419–431.

(7) Tweed, J.H. and Knott, J.F., Met. Sci., Vol. 17, 1983, pp. 45–54.

(8) Tweed, J.H. and Knott, J.F., Acta Metall., Vol. 35, 1987, pp. 1401–1414.

(9) McRobie, D.E. and Knott, J.F., Mater. Sci. Tech., Vol. 1, 1985, pp. 357–365.

(10) Goodier, J.N., Trans. ASME, Vol. 55, 1933, pp. 39–44.

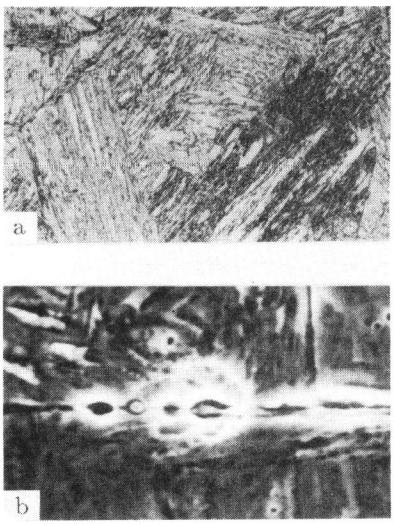

Fig. 1 As-quenched microstructure (a) and inclusions (b).

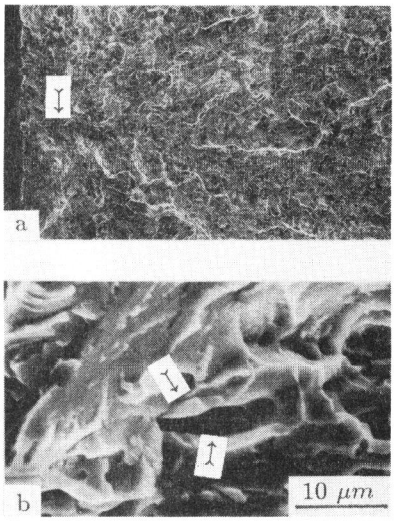

Fig. 2 Fracture initiation site (arrowed) in specimen M2 (a) and the inclusions (arrowed) in the site (b).

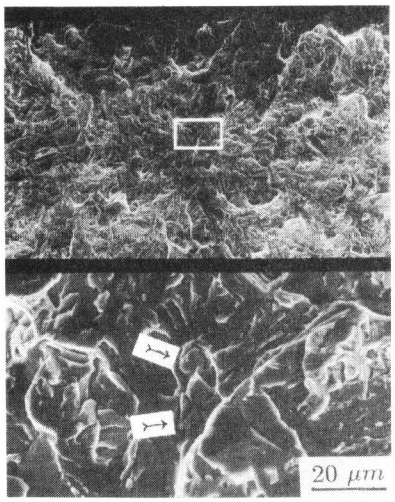

Fig. 3 Fracture initiation site in specimen M3 and the inclusions (arrowed) in the site.

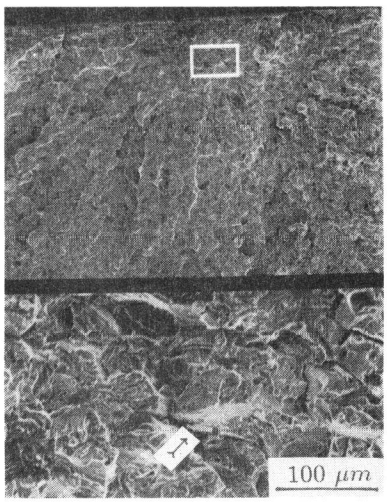

Fig. 4 Fracture initiation site in specimen M4 and the inclusion (arrowed) in the site.